

Effective L-Series Mass Absorption Coefficients for EDS

David G. Rickerby* and Norbert Wächter

IHCP, European Commission Joint Research Centre, 21020 Ispra (Varese), Italy

Abstract. Energy dispersive X-ray spectroscopy has insufficient resolution to separate the individual lines of low energy L-series peaks. However, the mass absorption coefficients for $L\alpha$ and $L\beta$ radiation differ significantly for elements with atomic numbers between 21 and 32. Effective mass absorption coefficients for the entire L-shell emission were determined by measuring the variation of the X-ray intensities emitted from pure element standards, as a function of the accelerating voltage, and fitting the experimental data with a theoretical curve using the XMAC software. These experimentally determined mass absorption coefficients were compared with average values calculated on the basis of the theoretical line intensities, taking into account the primary vacancy generation and the radiationless Coster-Kronig transitions.

Key words: Mass absorption coefficients; energy dispersive analysis; L-series.

The component lines of the L-series are not completely resolvable by energy dispersive spectrometry for X-ray energies less than approximately 3 keV. This results in the $L\alpha$ and $L\beta$ peaks appearing as a single peak with an energy shift ~ 10 eV with respect to the exact $L\alpha$ line position. Use of the undeconvoluted L peak for quantitative analysis may therefore lead to large errors in cases where mass absorption differs significantly for the individual lines [1–3]. The elements principally affected are those lying between atomic numbers 21 (scandium) and 32 (germanium), for which the energy of the $L\beta$ line is slightly greater than the ionization energy of the L_3 subshell. Due to the proximity of the absorption edge the mass absorption coefficients for $L\beta$

radiation in these elements are up to a factor of six higher than for $L\alpha$.

An additional source of error in analysis constitutes the uncertainty in the reported values of the mass absorption coefficients for the L lines of the elements from Ti to Zn [4–6]. The self absorption coefficient for atoms bonded with atoms of other elements can furthermore vary noticeably from that in the pure element because the electron transition probabilities and X-ray absorption properties are influenced by modifications in the structure of the valence band caused by alloying. The 3d transition elements, in which the valence band is incompletely filled, are most strongly affected and the self absorption of Ni $L\alpha$ in alloys such as Ni-Al or Ni-Zn, for example, is consequently weaker than in the pure metal [7, 8].

Because of the uncertainties in analysis using soft X-rays, a method has been developed to determine precise values for mass absorption coefficients by measuring the variation of the emitted line intensity with accelerating voltage. The experimentally measured values of the X-ray emission rate per unit beam current are compared to a theoretical curve computed by the XMAC software [8, 9], which is based on the XPP model of X-ray generation. Using an iterative procedure to optimize the fit a value for the mass absorption coefficient can be obtained.

Two alternative approaches may be used to perform quantitative energy dispersive analysis using compound L-series peaks. In the first, the $L\alpha$ intensity is estimated by multiplying the total intensity of the L-shell radiation by a relative intensity factor, a_L , corresponding to the ratio of the $L\alpha$ intensity to that emitted by the entire L-shell. In the second, the entire L-shell emission is considered [10] and the use of an

* To whom correspondence should be addressed

effective L-shell mass absorption coefficient is necessary [2]. Values of a_L have been determined experimentally [11, 12] and, provided that the mass absorption coefficients of $L\alpha$ and $L\beta$ radiation are similar, should be relatively independent of the accelerating voltage. Where this is not the case, a_L will depend strongly on the electron energy [3].

The present work discusses the experimental determination of effective mass absorption coefficients for L-series radiation for the elements between atomic numbers 22 and 33. These data will be compared with theoretical values derived from the probabilities of X-ray generation calculated from the radiative decay rates and effective vacancy distributions.

Experimental Procedure

Energy dispersive X-ray spectra were acquired with an Oxford Instruments Link Pentafet (Si-Li) detector, operated in the windowless mode, using an eXL II microanalysis system. The detector was installed on the column of a JEOL 6400F field emission scanning electron microscope. The energy resolution of the detector was 133 eV at Mn $K\alpha$ and the take off angle was 35 degrees. The pumping system of the microscope was equipped with a liquid nitrogen foreline trap and an activated alumina filter, allowing a final pressure of $2 \cdot 10^{-5}$ Pa to be achieved in the specimen chamber. The beam was rastered in the TV scanning mode, using a magnification of 100x, in an attempt to minimize the influence of hydrocarbon contamination [13]. Conditioning of the detector was carried out immediately before the experiments to remove the ice layer on the surface of the crystal. Spectra were obtained at eight different accelerating voltages between 5–30 kV for each of the elements of interest.

The standards employed were uncoated polished metal discs of > 99.9% purity mounted in a Geller UHV-compatible, type NM537F circular holder and a polished specimen of GaAs in an ASTIMEX METM25-44 metal mount. These standards were stored under vacuum before use to reduce oxidation of their surfaces. The electron beam current was monitored before and after spectrum acquisition by a pneumatically operated JEOL Probe Current Detector (PCD) connected to a Keithley Model 485 autoranging picoammeter. Beam currents were typically between 0.2 and 1.0 nA and were found to be stable to within about $\pm 1\%$ over a period of several minutes, with the microscope operated in the constant probe current mode. An acquisition live time of 200 s was used, while the dead time was generally in the range 30–40%. The total net X-ray counts above the linearly interpolated background were determined within an energy window defined between the channels at 1.5 times the FWHM on the low energy side of the Li line and 1.5 times the FWHM on the high energy side of the $L\alpha$ line.

Theory

An effective mass absorption coefficient for the total L-series emission can be estimated using the expression

$$\begin{aligned} (\mu/\rho)_L \approx & P_{L\alpha+L\eta+L\iota} (\mu/\rho)_{L\alpha} \\ & + (1 - P_{L\alpha+L\eta+L\iota}) (\mu/\rho)_{L\beta} \end{aligned} \quad (1)$$

where $P_{L\alpha+L\eta+L\iota}$ is the probability for generation of $L\alpha$, $L\eta$ and $L\iota$ X-rays, and it is assumed that the mass absorption coefficients for the $L\iota$ and $L\alpha$ radiation are approximately equal. The intensity of the $L\eta$ line can be considered negligible compared to the other emissions.

The probabilities of X-ray generation were those used by Röhrbacher et al. [3], obtained from the expressions

$$P_{L\alpha} = \frac{V_3\omega_3}{V_1\omega_1 + V_2\omega_2 + V_3\omega_3} \left[\frac{\Gamma_R(L_3M_{4,5})}{\Gamma_R(L_3)} \right] \quad (2)$$

for $L\alpha$ radiation and

$$\begin{aligned} P_{L\alpha+L\eta+L\iota} = & \frac{1}{V_1\omega_1 + V_2\omega_2 + V_3\omega_3} \\ & \left[V_3\omega_3 \frac{\Gamma_R(L_3M_{4,5}) + \Gamma_R(L_3M_1)}{\Gamma_R(L_3)} \right. \\ & \left. + V_2\omega_2 \frac{\Gamma_R(L_2M_1)}{\Gamma_R(L_2)} \right] \end{aligned} \quad (3)$$

for $L\alpha$, $L\eta$ and $L\iota$ radiation, where V_i is the effective vacancy distribution, ω_i is the fluorescence yield of the i th subshell and $\Gamma_R(L_iM_j)$ is the radiative decay rate of a vacancy from level L_i to level M_j . The atomic number dependent primary vacancy distributions were obtained from Schiebl et al. [14]. The fluorescence yields were taken from Krause [15] and the radiative decay rates from Schofield [16]. The effective vacancy distributions for the L_2 and L_3 subshells incorporate the effects of the radiationless Coster-Kronig transitions on the primary vacancy distribution.

Results and Discussion

Spectrum peaks for L-radiation obtained from pure Co and Cu standards are shown in Figs. 1 and 2, respectively. Contamination effects, evidenced by the presence of a small C K peak, are relatively minor. The contamination rate is $\sim 10^{-1} \text{ nm s}^{-1}$ for spot mode analysis [13] but $< 10^{-2} \text{ nm s}^{-1}$ in the scanning mode. The differences between the energies of the $L\alpha$ and $L\beta$ lines (0.775 and 0.790 keV for Co, 0.928 and 0.948 keV for Cu) are insufficient to allow the resolution of the individual lines by the spectrometer. The Co $L\iota$ peak at 0.678 keV and the Cu $L\iota$ peak at 0.811 keV are only partially resolved. The relative intensity of the $L\iota$ line with respect to $L\alpha$ decreases with increasing atomic number. For Ti and V the intensity of both these lines is of similar order of magnitude. Overlap with the O K line (0.523 keV), due to X-rays

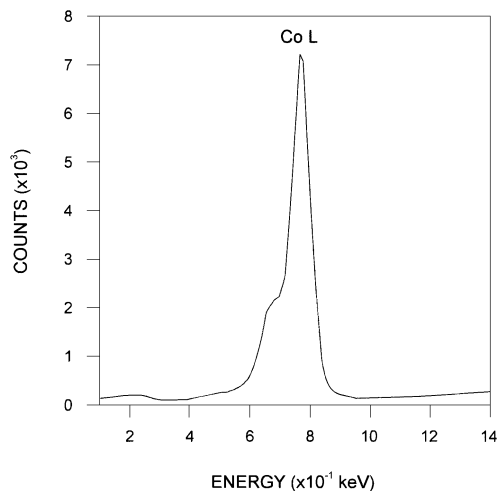


Fig. 1. Co L peak acquired at an accelerating voltage of 20 kV from a pure metal standard

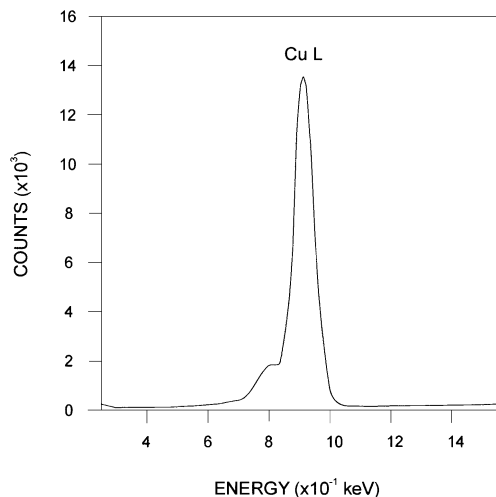


Fig. 2. Cu L peak acquired at an accelerating voltage of 20 kV from a pure metal standard

generated within the surface oxide layer on the metal standard, may cause difficulties with quantification for the Ti $L\alpha$ (0.452 keV), V $L\alpha$ (0.510 keV), Cr $L\alpha$ (0.573 keV) and Mn $L\beta$ (0.556 keV) peaks. Examination of the line shift for Cr $L\beta$ (~ 20 eV), together with AES analysis, has confirmed that a significant contribution to the overall peak intensity may arise from this source [17].

Figures 3 and 4 show experimental measurements of the X-ray emission rates per unit beam current as a function of the accelerating voltage for V L and Cu L radiation, respectively. Theoretical curves have been fitted to these data using the XMAC software, in order to determine the effective mass absorption coefficients

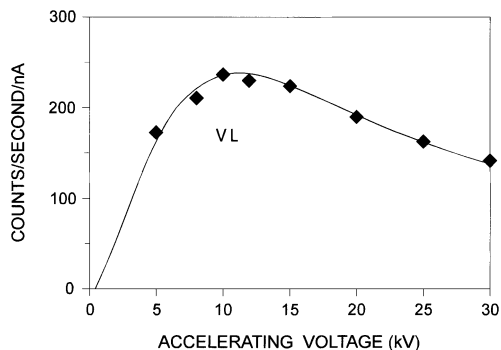


Fig. 3. Theoretical curve fitted to the experimental X-ray emission rate data for V L radiation using the XMAC software

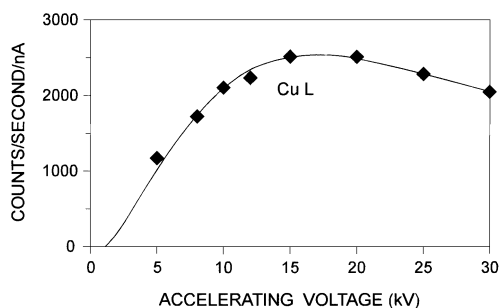


Fig. 4. Theoretical curve fitted to the experimental X-ray emission rate data for Cu L radiation using the XMAC software

for the L-peaks. The relative deviations of the experimental values from the theoretical curve, which were 1.21% for V L and 1.15% for Cu L , were $< 2\%$ for all the elements investigated. In performing the theoretical calculations it was assumed that the depth distribution curve was identical to that for the $L\alpha$ emission. Since the ionisation energies for the L-subshells are similar the depth distributions for $L\alpha$ and $L\beta$ should in any case be almost the same.

Table 1 lists the X-ray generation probabilities computed from equations 1 and 2, the $L\alpha$ and $L\beta$ mass absorption coefficients, $(\mu/\rho)_{L\alpha}$ and $(\mu/\rho)_{L\beta}$, and theoretical and measured values of the effective mass absorption coefficient, $(\mu/\rho)_{L\text{calc}}$ and $(\mu/\rho)_{L\text{meas}}$, for each element of interest. The difference between $P_{L\alpha+L\beta+L\gamma}$ and $P_{L\alpha}$ diminishes with increasing atomic number in accordance with the experimentally observed decrease in the relative intensity of the $L\beta$ line with respect to the overall peak intensity. Experimental measurements of the ratios of the $L\beta$ to $L\alpha$ line intensities for Mn, Fe, Co and Ni were larger than tabulated [17]. The theoretically computed values of the effective mass ab-

Table 1. X-ray generation probabilities [3] and $L\alpha$, $L\beta$ and effective L-series mass absorption coefficients ($\text{cm}^2 \text{g}^{-1}$) for the elements from Ti to As

Z	Element	$P_{L\alpha}$	$P_{L\alpha+L\eta+L\iota}$	$(\mu/\rho)_{L\alpha}$	$(\mu/\rho)_{L\beta}$	$(\mu/\rho)_{L\text{calc}}$	$(\mu/\rho)_{L\text{meas}}$
22	Ti			4550	26460		9311
23	V			4370	21888		5767
24	Cr			3850	19144		5460
25	Mn			3340	16282		3953
26	Fe	0.68778	0.77252	3350	14488	5884	4593
27	Co	0.71029	0.78366	3260	12465	5251	4162
28	Ni	0.71405	0.77588	3500	11379	5266	4494
29	Cu	0.71338	0.77034	1755	6750	2902	3270
30	Zn	0.71797	0.77031	1485	8547	3107	2223
31	Ga	0.71051	0.75789	1354	7341	2804	1802
32	Ge	0.70379	0.74626	1261	6474	2584	1996
33	As	0.69505	0.73603	1182	1109	1163	1435

sorption coefficient tend to overestimate the experimentally determined ones, except in the case of Cu. Theoretical values could not be determined for Ti, V, Cr and Mn because reliable estimates of the radiative decay rates were unavailable for elements of atomic number below 26.

The values for the $L\alpha$ and $L\beta$ mass absorption coefficients employed in the theoretical calculations and listed in Table 1 were those supplied for use with the STRATA [18] thin film analysis program. These values were obtained from the MAC86 compilation due to Heinrich [19] with certain modifications, in particular for the coefficients for self absorption of the $L\alpha$ lines from Sc to Cu and As $L\alpha$ in Ga [20]. Mass absorption coefficients determined by WDS using the XMAC software [8] are, in general, no more than 10% greater than these values and in many cases the error is less. However, as remarked previously, there is a wide variability in the reported values for the $L\alpha$ mass absorption coefficients. Some of this uncertainty results from measurements made on unresolved $L\alpha + L\beta$ peaks obtained by energy dispersive spectroscopy [6]. The values given by Henke [21] are consistently lower than those used here. If we assume values of $1915 \text{ cm}^2 \text{ g}^{-1}$ for Co $L\alpha$ and $11059 \text{ cm}^2 \text{ g}^{-1}$ for Co $L\beta$ [3] the theoretical effective mass absorption coefficient becomes $3893 \text{ cm}^2 \text{ g}^{-1}$ instead of $5251 \text{ cm}^2 \text{ g}^{-1}$. This is very near to the value of $3847 \text{ cm}^2 \text{ g}^{-1}$ that is found to yield the best results over a wide range of electron energies [22] and is also within 8% of the value of $4162 \text{ cm}^2 \text{ g}^{-1}$ determined in the present work.

Since the self absorption coefficients for As $L\alpha$ and $L\beta$ radiation are nearly the same the effective mass absorption coefficient for the L-series would be

expected to be similar to that for $L\alpha$, whereas the experimental measurements show that it is over 25% higher. The actual value, $1435 \text{ cm}^2 \text{ g}^{-1}$, is close to that of $1457 \text{ cm}^2 \text{ g}^{-1}$ for the $L\alpha$ mass absorption coefficient determined from WDS measurements on a GaAs standard.

The experimentally measured effective mass absorption coefficient for Ti L, $9311 \text{ cm}^2 \text{ g}^{-1}$, is lower than the value of $12680 \text{ cm}^2 \text{ g}^{-1}$ [2], which was found to give improved analysis results for a thin Ti layer deposited on Si. This may be due to the relative insensitivity of measurements on thin layers to differences in the mass absorption coefficient, or to the contribution of O K radiation emitted from the surface oxide layer on the standard to the apparent Ti $L\alpha$ intensity at low accelerating voltages. The spectra acquired from a pure Sc standard had inadequate signal to noise ratios to allow X-ray count rates to be measured with sufficient precision for determination of the effective L-shell mass absorption coefficient for this element.

Conclusions

- Experimentally determined effective L-series mass absorption coefficients for the elements between atomic numbers 22 and 32 are greater than those for $L\alpha$ radiation alone because of the contribution of the more strongly absorbed $L\beta$ line to the total L peak intensity.
- The experimental values are generally smaller than those predicted by a simple theoretical calculation based on the relative generation probabilities of the constituent X-ray lines.

- The experimental value of the effective mass absorption coefficient for the Co L peak is in reasonably close agreement with the value of $3847 \text{ cm}^2 \text{ g}^{-1}$ reported previously to give the most accurate analytical results over a range of electron energies.
- The principal source of error in these measurements, especially at low accelerating voltages, is the presence of oxide and carbon contamination layers on the standards.

Acknowledgements. The authors wish to thank K. Röhrbacher and his colleagues at the Technical University of Vienna for making available their theoretical calculations of the X-ray generation probabilities and R. G. Saint-Jacques for his comments on the manuscript.

References

- [1] D. G. Rickerby, J.-F. Thiot, *Mikrochim. Acta* **1994**, 114/115, 421.
- [2] D. G. Rickerby, *Microsc. Microanal. Microstruct* **1995**, 6, 621.
- [3] K. Röhrbacher, M. Andrae, P. Klein, J. Wernisch, *Mikrochim. Acta Suppl.* **1996**, 13, 507.
- [4] D. F. Kyser, *Proc. 6th Int. Congress X-Ray Optics and Microanalysis*. Tokyo University Press, 1972, p. 147.
- [5] J. I. Goldstein, D. E. Newbury, P. Echlin, D. C. Joy, C. Fiori, E. Lifshin, *Scanning Electron Microscopy and Microanalysis*. Plenum, New York, 2nd Edn. 1984, p. 313.
- [6] M. Watanabe, Z. Horita, M. Nemoto, *Electron Microscopy 1994, Proc. 13th. Int. Congress on Electron Microscopy. Paris, 1994*, Vol. 1, p. 605.
- [7] J.-L. Pouchou, F. Pichoir, *J. Microsc. Spectrosc. Electron.* **1985**, 10, 291.
- [8] J.-L. Pouchou, *Mikrochim. Acta Suppl.* **1996**, 13, 39.
- [9] J.-L. Pouchou, F. Pichoir, *Microbeam Analysis*. San Francisco Press, 1988, p. 319.
- [10] J. C. Russ, *Proc. 9th. Annual Conference of the Microbeam Analysis Society*. Ottawa, 1994, p. 22.
- [11] T. P. Schreiber, A. M. Wims, *Microbeam Analysis*. San Francisco Press, 1982, p. 317.
- [12] T. P. Schreiber, A. M. Wims, *X-Ray Spectram.* **1982**, 11, 42.
- [13] D. G. Rickerby, *Mikrochim. Acta Suppl.* **1996**, 13, 493.
- [14] C. Scheibl, J. Wernisch, *Scanning* **1993**, 15, 203.
- [15] M. O. Krause, *J. Phys. Ref. Data* **1979**, 8, 307.
- [16] J. H. Schofield, *Phys. Rev.* **1974**, A10, 1507.
- [17] G. L'Espérance, G. Botton, M. Caron, *Microbeam Analysis*. San Francisco Press, 1990, p. 284.
- [18] J.-L. Pouchou, F. Pichoir, *Electron Microscopy 92, Proc. 10th. European. Congress on Electron Microscopy*. Granada, 1992, Vol. 1, p. 293.
- [19] K. F. J. Heinrich, *Proc. 11th. Int. Congress X-Ray Optics and Microanalysis. Ontario 1987*, p. 67.
- [20] J.-L. Pouchou, F. Pichoir, in *Electron Probe Quantitation*. In: K. F. J. Heinrich, D. E. Newbury (Eds.) Plenum, New York, 1991, p. 31.
- [21] L. Henke, *Atomic Data and Nuclear Data Tables* **1982**, 27, 1.
- [22] C. Schiebl, L. Foster, A. Pfeiffer, A. Testoni, *Microbeam Analysis*. San Francisco Press, 1994, p. 199.